



# Adsorption of Chromium (VI) onto Metakaolin: Isotherms, Modelling and Optimization

Abdulhamid Hamza\*, Abubakar Mashood Alao, Mohammed Sani Galadima

Department of Chemical Engineering,  
 Ahmadu Bello University, Zaria, NIGERIA

\*Corresponding Author

DOI: <https://doi.org/10.30880/jst.2019.11.01.005>

Received 1 April 2019; Accepted 10 June 2019; Available online 20 June 2019

**Abstract:** This paper focuses on the application of metakaolin as an adsorbent for the removal of hexavalent chromium (Cr(VI)) from aqueous solution. Metakaolin was prepared and characterized using x-ray fluorescence spectroscopy (XRF), scanning electron microscopy (SEM), specific surface area and pH at point of zero charge analysis. Batch adsorption experiments were designed and conducted with the aid of the statistical central composite design in order to study the effects of pH (2–10), initial concentration of Cr(VI) (25–100 mg/L) and adsorbent dosage (2–10 mg/L). Adsorption of Cr(VI) onto metakaolin was described by a model quadratic equation. Analysis of variance revealed significance of the model quadratic equation. The predicted optimum values of the process variables were: pH of 2.48, initial Cr(VI) concentration of 32.16 mg/L and adsorbent dosage of 7.08 g/L. The experimental percentage adsorption of Cr(VI) obtained under the predicted optimum conditions (34.43 %) is very to the predicted value of 37.51 %. The adsorption equilibrium data were analyzed using Langmuir, Freundlich and Dubinin-Radushkevich isotherms. The adsorption equilibrium data is best described by the Freundlich isotherm. The maximum adsorption capacity ( $q_{max}$ ) for Cr(VI) adsorption onto metakaolin is 6.36 mg/g. The results showed that metakaolin is a promising adsorbent for the removal of hexavalent chromium from water.

**Keywords:** Adsorption, metakaolin, hexavalent chromium, isotherms, optimization.

## 1. Introduction

Contamination of water bodies by heavy metals poses serious threats to public health in many countries. Heavy metals such as chromium, lead, cadmium, and mercury are toxic, non-biodegradable, soluble in water and persistent in the biogeosphere [1, 2]. In water, chromium mainly exists in two oxidation states: trivalent chromium (Cr(III)) and hexavalent chromium (Cr(VI)). Hexavalent chromium is much more toxic than the trivalent chromium [3]. Hexavalent chromium affects kidneys, respiratory system, eyes, skin and liver. The International Agency for Research on Cancer (IARC) listed Cr(VI) as a group I human carcinogen [4]. According to the World Health Organization (WHO), the recommended a maximum concentration of Cr(VI) in drinking water is 0.05 mg/L. The  $LD_{50}$  for Cr(VI) is in the range of 50 to 150 mg/kg [5].

Various water and wastewater treatment technologies (such as sedimentation, chemical precipitation, ion exchange, reverse osmosis, membrane filtration, adsorption, biochemical treatment, advanced oxidation processes, etc) have been used for the removal of Cr(VI) from water [6, 7]. Each technology has its own inherent limitations such as complexity, high cost, high energy input, generation of sludge, etc. Adsorption is a simple and effective technology for

the removal of trace amounts of various heavy metals from water. Activated carbon is the most widely used adsorbent due to its high specific surface area and high chemical stability. However, commercial activated carbon is expensive, and it is often difficult to separate and recover the activated carbon from the treated water. Therefore, there is a need to develop effective and cheaper adsorbents that could complement or replace activated carbon in the adsorption process [8, 9].

There has been a lot of research interest on developing cheap adsorbents from various clays because clays are cheap, non-toxic and chemically stable [8, 10]. Kaolin is one of the most abundant clays with high chemical stability and low expansion coefficient [8, 11, 12]. The potential of kaolin for adsorption of various heavy metals in water has been reported by various researchers [11-14]. However, kaolin is characterized by small specific surface area of 10 to 20 m<sup>2</sup>/g and low cation exchange capacity of 3–15 meq/100g of clay [14]. This limits the application of kaolin as an adsorbent. On the other hand, the adsorption properties of clays can be enhanced by modifying their structures and chemical compositions using various chemical additives and thermal treatment [15].

Calcination of clays often leads to loss of the crystalline structure of the clays. The calcined clays usually exhibit higher specific surface areas and adsorption capacities when compared with the raw clays [8, 16]. Metakaolin is the dehydroxylated amorphous form of kaolin that is obtained by calcination of kaolin at a temperature range of 500°C to 800°C [8, 17]. There have been some works on the adsorption of Cr(VI) onto kaolin [12, 13, 15, 18]. However, there are very limited works on the adsorption of heavy metals, especially Cr(VI) onto metakaolin [8]. Hence, present work was aimed at investigating adsorption of Cr(VI) onto metakaolin. The effects of pH, initial concentration of Cr(VI) and adsorbent dosage on the adsorption process were studied using the response surface methodology (RSM) in order to develop a model equation for the adsorption process and optimize the process. The adsorption isotherms were also studied under the optimum conditions of the process.

## 2. Materials and Method

### 2.1 Materials

White kaolin was sourced from Kankara village in Katsina state, Nigeria. The raw kaolin was beneficiated in order to remove impurities. The kaolin was beneficiated and calcined at 700 °C for two hours in Nabertherm furnace to yield metakaolin [19]. The morphology of the metakaolin was studied using Phenom Pro-X scanning electron microscope (SEM). Minipal-4 x-ray fluorescence spectrometer was used to determine the chemical composition of the metakaolin. The specific surface area of the metakaolin was determined using the Sear's method [20]. The pH at point of zero charge of the metakaolin was measured using the salt titration method [21].

### 2.2 Adsorption Experiments

1000 mg of K<sub>2</sub>Cr<sub>2</sub>O<sub>7</sub> was dissolved in 1 L of distilled water to obtain the stock solution of Cr(VI). The pH of Cr(VI) solutions was adjusted using either HCl or NaOH solution. Adsorption experiments were carried out by shaking 100 mL of Cr(VI) solution of the desired concentration with the required amount of the metakaolin adsorbent. The flasks were continuously shaken for the desired contact time. Thereafter, the adsorbent was separated via filtration. The concentration of the Cr(VI) in the filtrate was determined using an atomic absorption spectrophotometer (AAS 500, England). The percentage adsorption of Cr(VI) onto metakaolin and equilibrium adsorption capacity (q<sub>e</sub>) of the adsorbents for Cr(VI) were calculated using Eqs. 1 and 2, respectively.

$$\% \text{ Adsorption} = \frac{C_0 - C_t}{C_0} \times 100\% \quad (1)$$

$$q_e = \frac{(C_0 - C_e)V}{m} \quad (2)$$

where C<sub>0</sub> is the initial concentration (mg/L) of Cr(VI); C<sub>t</sub> is the concentration of Cr(VI) (mg/L) after contact time, t; C<sub>e</sub> is the concentration of Cr(VI) (mg/L) at equilibrium; m and V are the mass (g) of the metakaolin and volume (L) of the Cr(VI) solution, respectively.

### 2.3 Design of Adsorption Experiments

The effects of three process parameters (pH, initial concentration of Cr(VI) and adsorbent dosage) on the adsorption of Cr(VI) onto metakaolin were investigated using the central composite design as implemented in the Design Expert software. The lowest and highest levels of each independent variable are given in Table 1. In this work,

the response is the percentage adsorption of Cr(VI). Based on experimental results obtained, an empirical relationship between the response and independent variables was fitted to second order polynomial.

**Table 1 - Experimental ranges of the investigated independent variables.**

Independent variable	Code	Ranges		
		Lowest	Middle	Highest
pH	A	2	6	10
Initial concentration of Cr(VI) (mg/L)	B	25	62.5	100
Adsorbent dosage (g/L)	C	2	6	10

### 3. Results and Discussion

#### 3.1 Characterization of the metakaolin

Table 2 presents the chemical composition of the raw kaolin, beneficiated kaolin and the metakaolin produced. The Si/Al ratio of the raw kaolin was initially 1.90 which decreased slightly to 1.86 after beneficiation. The decrease in the Si/Al ratio could be attributed to washing away of free silica during the beneficiation process. The decrease in loss on ignition (LoI) after metakaolinization could be attributed to dehydroxylation of the clay during the calcination process, leading to removal of chemically combined water in the clay [17]. As shown in Fig. 1a, the beneficiated kaolin has a booklet morphology. Fig. 1b shows that the booklet morphology of the beneficiated kaolin has been lost after metakaolinization due to breaking down of the crystalline kaolinite structure. The metakaolin has a lump – like morphology which could be attributed to its amorphous nature [19]. The measured specific surface area of the metakaolin is 24.60 m<sup>2</sup>/g which is higher than that of the beneficiated kaolin (17.40 m<sup>2</sup>/g). The increase in the specific surface area is due to the loss of crystallinity of the kaolin upon calcination [16, 17]. The measured pH at point of zero charge of the metakaolin is 5.80.

**Table 2 - Chemical composition (wt %) of Kankara kaolin and metakaolin**

Component	Raw Kaolin	Beneficiated Kaolin	Metakaolin
SiO <sub>2</sub>	54.36	51.08	57.23
Al <sub>2</sub> O <sub>3</sub>	28.58	26.93	31.83
Na <sub>2</sub> O	0.32	0.55	0.28
K <sub>2</sub> O	3.84	1.72	1.72
MgO	0.39	0.43	0.48
CaO	1.93	1.24	1.39
CuO	0.03	0.03	0.02
TiO <sub>2</sub>	0.13	0.14	0.16
Fe <sub>2</sub> O <sub>3</sub>	0.75	0.91	1.74
LoI	8.76	14.31	1.56
SiO <sub>2</sub> /Al <sub>2</sub> O <sub>3</sub>	1.90	1.86	1.79

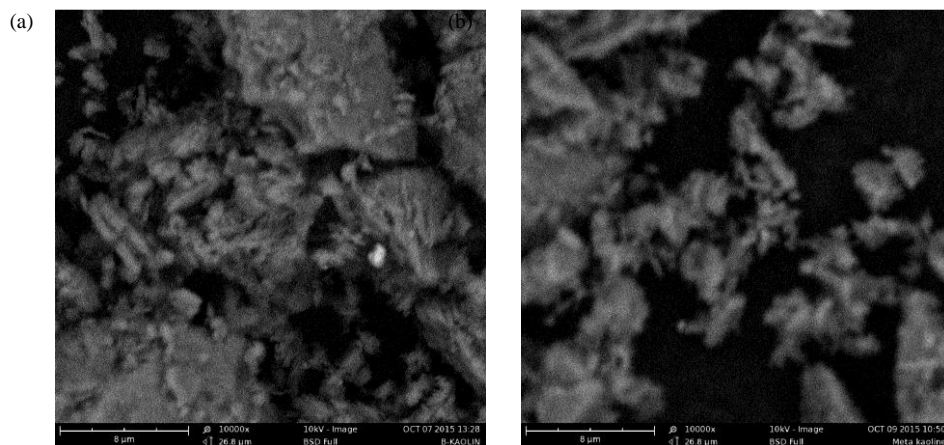


**Fig. 1 - SEM images of (a) the beneficiated kaolin, and (b) the metakaolin.**

### 3.2 Adsorption of Cr(VI) onto Metakaolin

Fig. 2 shows that the percentage adsorption of Cr(VI) onto metakaolin increases with increase in contact time up to 120 minutes. The adsorption was first in the beginning due to the larger surface area of the adsorbent and high driving force at the beginning of the adsorption process [14]. Adsorption equilibrium was achieved after 120 minutes. Therefore, all subsequent experiments in this work were carried out for 120 minutes.

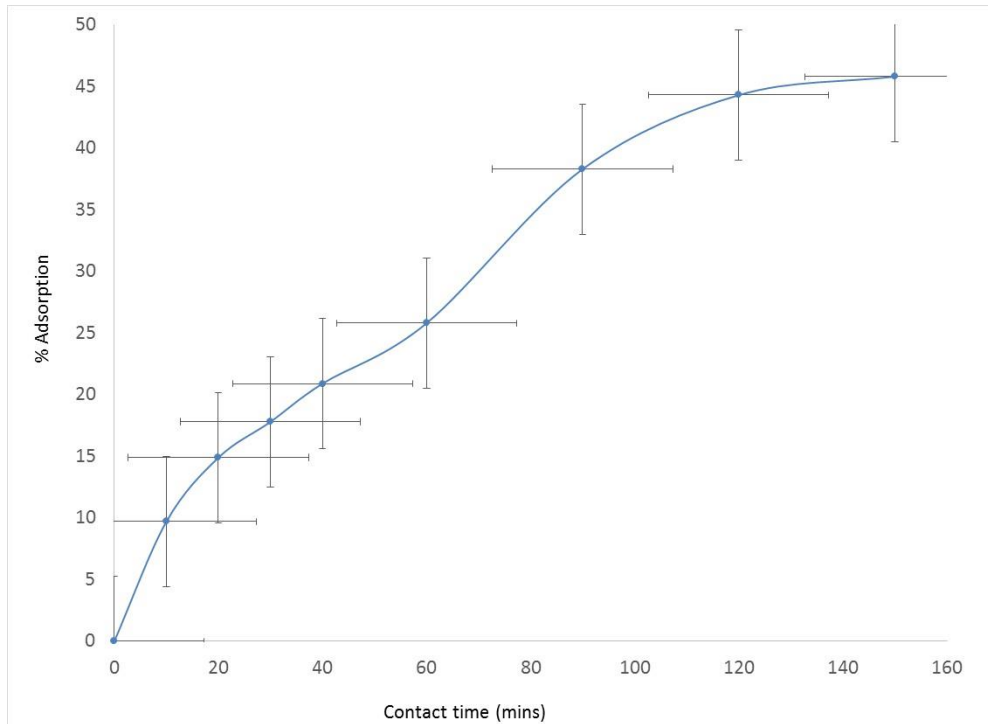


Fig. 2 - Effect of contact time on percentage adsorption of Cr(VI) adsorption onto metakaolin.

### 3.3 Modelling of Cr(VI) adsorption onto metakaolin

The central composite design matrix including the experimental results obtained for Cr(VI) adsorption onto metakaolin are presented in Table 3. The second order quadratic model equation (Eq. 3) that links the response (percentage adsorption) and the independent variables (pH, initial concentration of Cr(VI), and adsorbent dosage abbreviated by A, B and C, respectively) was suggested by the Design Expert software.

$$\text{Adsorption} = 31.21 - 1.95A + 6.45B + 4.03C - 0.92A^2 + 3.97B^2 + 5.38C^2 - 2.27AB - 2.23AC + 0.37BC \quad (3)$$

The suitability of the suggested quadratic model equation for navigating the design space in terms of percentage adsorption of Cr(VI) was ascertained using analysis of variance (ANOVA) of the suggested model equation. The results of the analysis are presented in Table 4, from where it is seen that the suggested model equation is significant with F-value of 30.91 and p-value below 0.05. Adequate precision is a measure of signal to noise ratio. A minimum ratio of 4 is desirable for adequate precision [22, 23]. Herein, the adequate precision of 18.163 indicates an adequate signal. Hence, the model quadratic equation is reliable and can be used to navigate the design space. The lack of fit F-value of 3.93 and p-value of 0.156 implies that the lack of fit is not significant relative to the pure error. The correlation coefficient of the model ( $R^2$ ) is 0.9578. This means that 95% of the total variation in Cr(VI) adsorption onto metakaolin is adequately represented by the model quadratic equation.

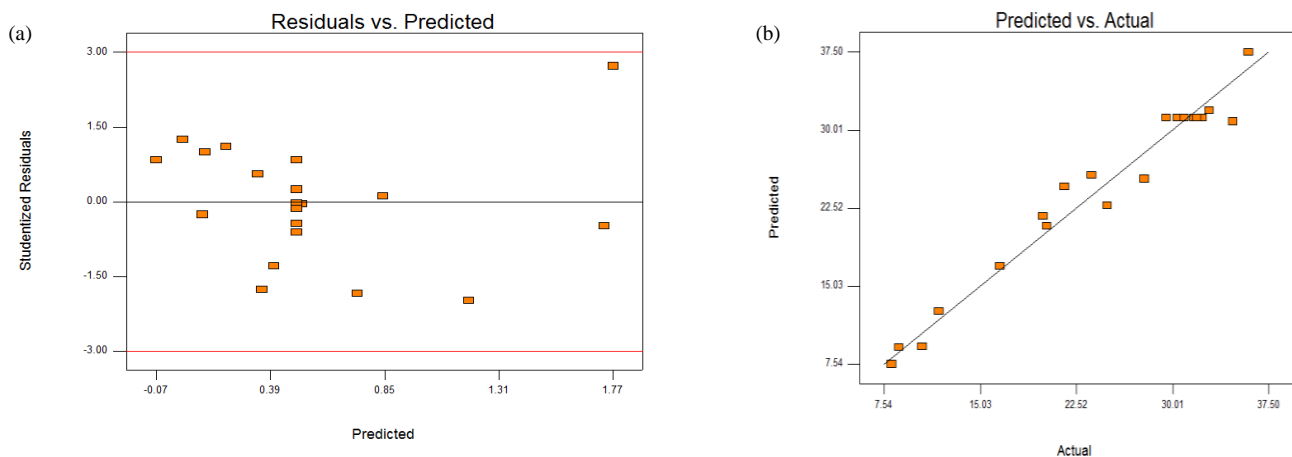
The plot of studentized residuals against predicted percentage Cr(VI) adsorption is shown in Fig. 3a. Based on the random scattering of the points, the variance of the original observations can be considered to be constant for all values of the response [23]. The random scattering of the experimental points also indicates the lack of need for transformation of the experimental values which confirms the validity of the model employed. Fig. 3b shows the plot of the experimentally determined responses (actual values) against responses obtained from the developed model quadratic equation (the predicted values). The plot shows good correlation between the actual and the predicted results; this indicates reliability of the model quadratic equation to predict the response at various values of the independent variables.

**Table 3 - Central composite design matrix with the experimental responses for Cr (VI) adsorption onto metakaolin**

Run	pH	Initial Concentration of Cr(VI) (mg/L)	Adsorbent dose (g/L)	Percentage adsorption (%)
1	10.00	100.00	10.00	16.56
2	10.00	25.00	10.00	20.22
3	5.50	62.50	12.73	24.90
4	5.50	62.50	6.00	30.40
5	2.07	62.50	6.00	34.70
6	5.50	62.50	6.00	29.50
7	5.50	62.50	6.00	31.67
8	1.00	100.00	10.00	21.60
9	5.50	125.57	6.00	27.80
10	1.00	25.00	2.00	23.70
11	1.00	25.00	10.00	35.92
12	13.07	62.50	6.00	8.71
13	10.00	100.00	2.00	11.80
14	10.00	25.00	2.00	8.12
15	5.50	62.50	6.00	31.90
16	5.50	62.50	6.00	32.30
17	5.50	62.50	0.73	10.50
18	5.50	0.57	6.00	32.86
19	1.00	100.00	2.00	19.91
20	5.50	62.50	6.00	30.93

**Table 4 - Analysis of variance results for Cr (VI) adsorption onto metakaolin**

Source	Sum of Squares	Degree of Freedom	Mean Squares	F-value	P-value
Model	1513.74	9	168.19	30.91	0.0001
A	51.81	1	51.81	9.52	0.0115
B	568.84	1	568.84	104.53	0.0001
C	221.4	1	221.4	40.68	0.0001
A <sup>2</sup>	12.18	1	12.18	2.24	0.1655
B <sup>2</sup>	226.99	1	226.99	41.71	0.0001
C <sup>2</sup>	417.86	1	417.86	76.79	0.0001
AB	41.09	1	41.09	7.55	0.0206
AC	39.92	1	39.92	7.34	0.0220
BC	1.09	1	1.09	0.20	0.0443
Lack of Fit	48.94	5	9.79	3.93	0.1560

**Fig. 3 - Plots of (a) Studentized residuals against predicted percentage adsorption of Cr(VI), (b) Predicted against the actual experimental values of percentage adsorption of Cr(VI).**

### 3.4 Effect of Process Variables on Adsorption of Cr(VI) onto Metakaolin

The perturbation plots displayed in Fig. 4 compare the effects of the three independent variables on the response at the central point (pH = 6, initial Cr(VI) concentration = 62.5 mg/L, adsorbent dosage = 6 g/L). The perturbation plots were made by changing only one variable over its range given in Table 1 while keeping the other variables constant. As apparent in Fig. 4, the response decreases with an increase in pH (A) and the initial Cr(VI) concentration (B). By looking at the slopes of pH and initial Cr(VI) concentration, it can be concluded that the response is more sensitive to pH than to the initial Cr(VI) concentration. On the other hand, the curvature of the perturbation plot for adsorbent dosage (C) indicates that the response increases with increase in the adsorbent dosage up to a certain level and then decreases. It shall be noted that the perturbation plots show the effects of each of the three independent variables individually. As shown in Table 3, the interactions between independent variables are significant with p-values below 0.05. The interactions between the independent variables can be explained using the 3D response surface plots presented in Fig. 5.

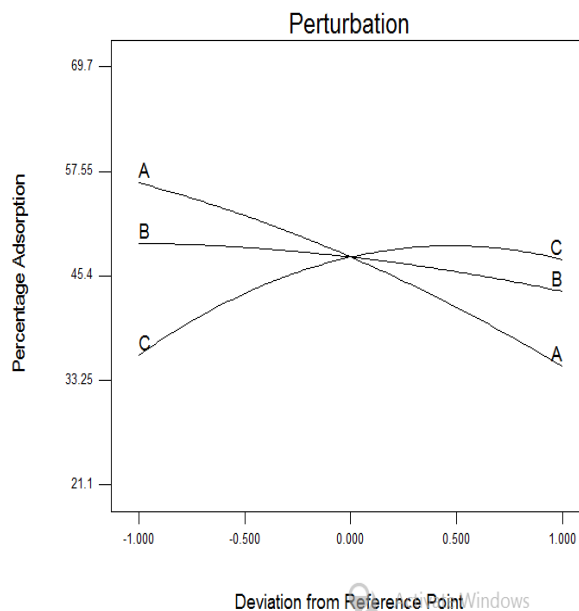
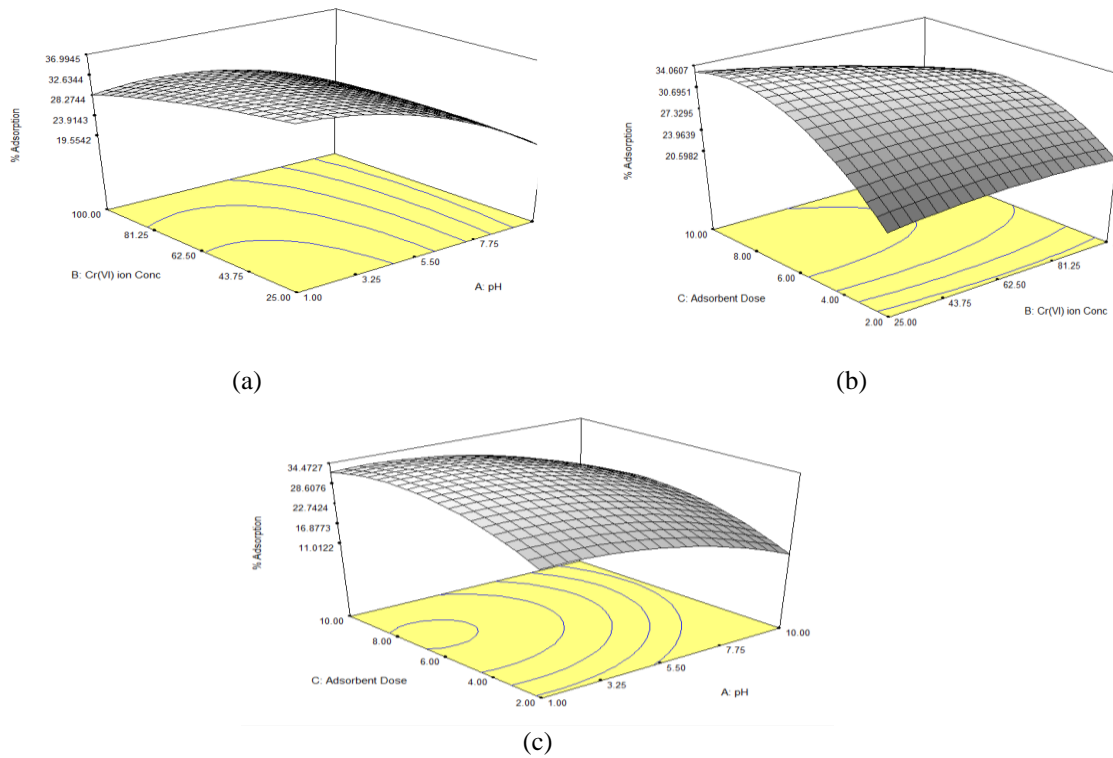


Fig. 4 - Perturbation plots for the adsorption of Cr(VI) onto metakaolin.

Fig. 5a depicts the combined effect of pH and initial Cr(VI) concentration on the percentage adsorption of Cr(VI). The percentage adsorption of Cr(VI) ion increases slightly with decrease in the initial concentration of Cr(VI) ions. This can be explained by the fact that all adsorbents have a limited number of active binding sites, and at a certain concentration the active sites become saturated [24]. It is apparent in Figs 5a and 5c that the adsorption increases with decrease in the solution pH. Generally, at solution pH below pH at point of zero charge, an adsorbent has positive surface charge and can readily adsorb negatively charged species from solution. While at pH above pH at point of zero charge the surface charge of an adsorbent is negative, so it can readily adsorb positively charged species from solution. At low solution pH, the predominant Cr(VI) species are  $\text{HCrO}_4^-$  and  $\text{Cr}_2\text{O}_7^{2-}$  and above neutral pH only  $\text{CrO}_4^{2-}$  is stable [25]. At low pH, the surface of metakaolin is positively charged since the measured pH at point of zero charge of metakaolin is 5.80. Hence, there is an electrostatic attraction between the surface of metakaolin and the negatively charged Cr(VI) ions which leads to higher adsorption. When the solution pH is greater than the pH of point zero charge of metakaolin, the surface of metakaolin is negatively charged. Hence, the negatively charged surface of metakaolin repels anionic species of chromium leading to reduced adsorption of Cr(VI) ions. Moreover, in acidic medium, the surface of metakaolin is protonated. The protonation favours adsorption of Cr(VI) in the anionic forms onto metakaolin [26]. As the solution pH is raised, the degree of protonation of the surface of metakaolin decreases leading to reduced adsorption of Cr(VI).

Furthermore, there is competition between  $\text{OH}^-$  and  $\text{CrO}_4^{2-}$  in alkaline medium. The reduction in net positive surface charge of metakaolin causes weakening of electrostatic forces between Cr(VI) species and metakaolin, which eventually leads to reduced percentage adsorption at high solution pH. Figs. 5b and 5c show that the percentage adsorption of Cr(VI) increases with increase in the metakaolin dosage. The number of surface active sites of an adsorbent increases as the dose of adsorbent increases, thereby enhancing percentage adsorption of Cr(VI) onto metakaolin. However, when the adsorbent dosage exceeds the optimum value of about 7 g/L, percentage adsorption of Cr(VI) begins to decline due to aggregation of metakaolin particles which decreases of the exposed surface area of metakaolin [27].



**Fig. 5 - 3D response surface plots for Cr(VI) adsorption onto metakaolin showing the simultaneous effects of (a) pH and initial concentration of Cr(VI), (b) adsorbent dose and initial concentration of Cr(VI) and (c) (b) pH and adsorbent dose.**

The results of ANOVA presented in Table 4 shows that the p-values of the interaction terms (AB, BC and AC) are less than 0.05; hence, there are significant interactions between the three independent variables. These interactions can be seen in Fig. 5. Thus, Fig. 5a shows that decrease in pH causes a greater increase in Cr(VI) adsorption at a low initial concentration of Cr(VI) than at higher initial concentration of Cr(VI). Similarly, Fig. 5b indicates that Cr(VI) adsorption is more sensitive to pH when the adsorbent dosage is at its optimum level (7-8 g/L) than when the adsorbent is lower or higher than the optimum adsorbent dosage. Increase in adsorbent dosage at low pH will promote protonation of the adsorbent surface, leading to more electrostatic attraction between the negatively charged ions of chromium and positively charged surface of metakaolin. This will enhance the adsorption of Cr(VI) at low pH and high adsorbent dosage. Fig. 5a shows that the effect of the adsorbent dosage is more pronounced at a lower initial concentration of Cr(VI) due to greater availability of active adsorption sites at a lower initial concentration of Cr(VI) [27, 28].

### 3.5 Optimization of adsorption of Cr(VI) onto metakaolin

In this work, the optimization was targeted at maximizing the percentage adsorption of Cr(VI) by setting the process variables (pH, Initial concentration of Cr(VI) and adsorbent dose) within the studied ranges given in Table 1. The Design expert software was used to optimize the response through maximization of a function called the desirability function. When desirability functions became unity, the software searches for various conditions under which, the desirability function is maximized [29]. 37.51 % percentage adsorption of Cr(VI) was predicted at a pH of 2.48, initial Cr(VI) concentration and adsorbent dosage of 32.16 mg/L and 7.08 g/L, respectively. In order to verify the optimization results, experiments were performed under the predicted conditions (pH of 2.48, initial Cr(VI) concentration of 32.16 mg/L and adsorbent dosage of 7.08 g/L). The experimental percentage adsorption of Cr(VI) obtained under these conditions was 34.43 %. The good agreement between the experimental percentage adsorption of Cr(VI) and the predicted percentage adsorption validates the developed model.

### 3.6 Adsorption isotherms

Adsorption isotherms show the relationships between the concentration of adsorbate on the solid adsorbent phase and its concentration in the liquid phase at equilibrium. Isotherms provide information about the capacity of adsorbents and the mechanism of adsorption. Three adsorption isotherm models namely, Langmuir, Freundlich and Dubinin-Radushkevich isotherms were selected in this study [30]. The linearized forms of the Langmuir, the Freundlich and the Dubinin-Radushkevich isotherms are given by Eq. 4, 5 and 6 respectively:

$$\frac{C_e}{q_e} = \frac{1}{q_{\max} K_L} + \frac{C_e}{q_{\max}} \tag{4}$$

$$\ln q_e = \ln K_F + \frac{1}{n} \ln C_e \tag{5}$$

$$\ln q_e = \ln Q_S - K_D \varepsilon^2 \tag{6}$$

where  $C_e$  is the equilibrium concentration of the Cr(VI) ions in solution,  $q_{\max}$  is the Langmuir maximum adsorption capacity of metakaolin,  $K_L$  is the Langmuir constant that is related to the energy of adsorption, respectively.  $K_F$  and  $n$  are the Freundlich adsorption isotherm constants which determine the extent of the adsorption process, and the degree of nonlinearity between solution concentration and adsorption, respectively.  $Q_s$  is the Dubinin-Radushkevich maximum adsorption capacity,  $K_D$  is the activity coefficient which indicates the mean adsorption energy (E).  $\varepsilon$  is the Polanyi potential which is calculated using Eq. 7. The mean adsorption energy (E) is calculated using Eq. 8.

$$\varepsilon = RT \ln(1 + 1/C_e) \tag{7}$$

$$E = \frac{1}{\sqrt{2K_D}} \tag{8}$$

Shown in Fig. 6 are the linearized plots of the three isotherms. Table 5 presents the isotherm parameters and correlation coefficients ( $R^2$ ) that were derived from the slopes and intercepts of the plots. By comparing the regression coefficients, adsorption of Cr(VI) onto metakaolin is best described by the Freundlich isotherm with  $R^2$  of 0.976. Therefore, adsorption of Cr(VI) involves formation of multiple layers of the adsorbed Cr(VI) ions on the surface of metakaolin. Other studies also reported that the Freundlich model described a much better fit than the Langmuir model in relation to Cr(VI) adsorption [12, 31, 32]. In addition, the constant ‘n’ in the Freundlich model ranges between 1.87 – 2.5, which further reveals favourability of metakaolin for Cr(VI) removal [33, 34].

Langmuir model also fitted the adsorption equilibrium data with  $R^2$  of 0.879. As seen in Table 6, the Langmuir maximum capacity ( $q_{\max}$ ) for Cr(VI) adsorption onto metakaolin is 6.36 mg/g. This adsorption capacity for Cr(VI) is substantially higher than that of the commercial kaolin (0.571 mg/g) reported by Ajouyed et al. [12]. Based on the results obtained from the Dubinin-Radushkevich model in Table 6, the mean free energy, E, of 0.1118 kJ/mol indicates that adsorption Cr(VI) ions onto metakaolin is mainly physisorption because when a mean free energy is less than 8 kJ/mol, physisorption controls the adsorption mechanism, while chemisorption prevails when the mean free energy is in the range of 8 and 16 kJ/mol [35].

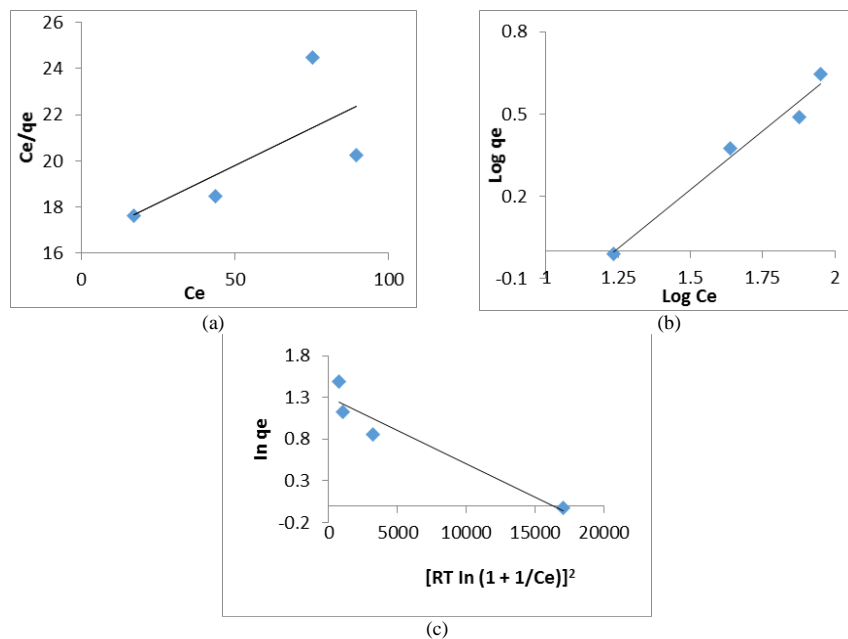


**Fig. 6 - Linearized plots of the adsorption isotherms for Cr(VI) adsorption onto metakaolin: (a) Langmuir isotherm, (b) Freundlich isotherm and (c) Dubinin-Radushkevich isotherm.**

**Table 5- Isotherm parameters for Cr(VI) adsorption onto metakaolin.**

Isotherm	Parameters	Values
Langmuir	$q_{\max}$	6.36 mg/g
	$R^2$	0.879
Freundlich	$K_F$	0.086
	$1/n$	0.4321
	$R^2$	0.976
Dubinin-Radushkevich	E	0.1118 kJ/mol
	$Q_D$	3.8 mg/g
	$R^2$	0.917

#### 4. Conclusion

The prepared metakaolin is amorphous with a specific surface area of 24.60 m<sup>2</sup>/g and a point of zero charge of 5.80. The adsorption-desorption equilibrium of Cr(VI) onto metakaolin was achieved after a contact time of 120 minutes. A model quadratic equation was developed for the adsorption of Cr(VI) onto metakaolin. Adsorption of Cr(VI) onto metakaolin is more sensitive to pH than to the initial Cr(VI) concentration and the adsorbent dosage. There are significant interactions between the three independent variables studied. The predicted optimum values of the process variables are: pH of 2.48, initial Cr(VI) concentration of 32.16 mg/L and adsorbent dosage of 7.08 g/L. The experimental percentage adsorption of Cr(VI) obtained under the predicted optimum conditions (34.43 %) is very close to the predicted value of 37.51 %. The adsorption equilibrium data is best described by the Freundlich isotherm. The maximum adsorption capacity ( $q_{\max}$ ) for Cr(VI) adsorption onto metakaolin is 6.36 mg/g.

#### References

- [1] Carolin, C.F., Kumar, P.S., Saravanan, A., Joshiba, G.J. & Naushad, M. (2017). Efficient techniques for the removal of toxic heavy metals from aquatic environment: A review. *Journal of Environmental Chemical Engineering*, 5(3), 2782-2799.
- [2] Wang, G., Zhang, S., Zhong, Q., Xu, X., Li, T., Jia, Y., Zhang, Y., Peijnenburg, W.J. & Vijver, M.G. (2018). Effect of soil washing with biodegradable chelators on the toxicity of residual metals and soil biological properties. *Science of the Total Environment*, 625, 1021-1029.
- [3] Bachate, S.P., Nandre, V.S., Ghatpande, N.S. & Kodam, K.M. (2013). Simultaneous reduction of Cr (VI) and oxidation of As (III) by *Bacillus firmus* TE7 isolated from tannery effluent. *Chemosphere*, 90(8), 2273-2278.
- [4] Tseng, C.-H., Lei, C. & Chen, Y.-C. (2018). Evaluating the health costs of oral hexavalent chromium exposure from water pollution: A case study in Taiwan. *Journal of Cleaner Production*, 172, 819-826.
- [5] Mohod, C.V. & Dhote, J. (2013). Review of heavy metals in drinking water and their effect on human health. *International Journal of Innovative Research in Science, Engineering and Technology*, 2(7), 2992-2996.
- [6] Burakov, A.E., Galunin, E.V., Burakova, I.V., Kucherova, A.E., Agarwal, S., Tkachev, A.G. & Gupta, V.K. (2018). Adsorption of heavy metals on conventional and nanostructured materials for wastewater treatment purposes: A review. *Ecotoxicology and Environmental Safety*, 148, 702-712.
- [7] Fu, F. & Wang, Q. (2011). Removal of heavy metal ions from wastewaters: a review. *Journal of Environmental Management*, 92(3), 407-418.
- [8] Uddin, M.K. (2017). A review on the adsorption of heavy metals by clay minerals, with special focus on the past decade. *Chemical Engineering Journal*, 308, 438-462.
- [9] Afroze, S. & Sen, T.K. (2018). A Review on Heavy Metal Ions and Dye Adsorption from Water by Agricultural Solid Waste Adsorbents. *Water, Air, & Soil Pollution*, 229(7), 225.
- [10] Bhattacharyya, K.G. & Gupta, S.S. (2008). Adsorption of a few heavy metals on natural and modified kaolinite and montmorillonite: a review. *Advances in Colloid and Interface Science*, 140(2), 114-131.
- [11] Bhattacharyya, K.G. & Sen Gupta, S. (2006). Adsorption of chromium (VI) from water by clays. *Industrial & engineering chemistry research*, 45(21), 7232-7240.
- [12] Ajouyed, O., Hurel, C. & Marmier, N. (2011). Evaluation of the adsorption of hexavalent chromium on kaolinite and illite. *Journal of Environmental Protection*, 2(10), 1347.
- [13] Li, Y., Yue, Q.-Y. & Gao, B.-Y. (2010). Effect of humic acid on the Cr (VI) adsorption onto Kaolin. *Applied Clay Science*, 48(3), 481-484.
- [14] Adebowale, K.O., Unuabonah, I.E. & Olu-Owolabi, B.I. (2006). The effect of some operating variables on the adsorption of lead and cadmium ions on kaolinite clay. *Journal of Hazardous Materials*, 134(1-3), 130-139.
- [15] Hezil, N., Fellah, M., Assala, O., Touhami, M.Z. & Guerfi, K. (2018) Elimination of Chromium (VI) by Adsorption onto Natural and/or Modified Kaolinite, pp. 106-112, *Trans Tech Publ*.
- [16] San Cristóbal, A.G., Castelló, R., Luengo, M.A.M. & Vizcayno, C. (2009). Acid activation of mechanically and thermally modified kaolins. *Materials Research Bulletin*, 44(11), 2103-2111.

- [17] Edomwonyi-Otu, L., Aderemi, B.O., Ahmed, A.S., Coville, N.J. & Maaza, M. (2013). Influence of thermal treatment on Kankara kaolinite. *Opticon*1826, (15).
- [18] Deng, L., Shi, Z., Luo, L., Chen, S.-y., Yang, L.-f., Yang, X.-z. & Liu, L.-s. (2014). Adsorption of hexavalent chromium onto kaolin clay based adsorbent. *Journal of Central South University*, 21(10), 3918-3926.
- [19] Salahudeen, N. (2018). Metakaolinization Effect on the Thermal and Physiochemical Properties of Kankara Kaolin. *KMUTNB International Journal of Applied Science and Technology*, 11(2), 127-135.
- [20] Maaref, S., Kantzas, A. & Bryant, S.L. (2019). The Effect of Silanization Assisted Nanoparticle Hydrophobicity on Emulsion Stability through Droplet Size Distribution Analysis. *Chemical Engineering Science*.
- [21] Tan, W.-f., Lu, S.-j., Liu, F., Feng, X.-h., He, J.-z. & Koopal, L.K. (2008). Determination of the point-of-zero charge of manganese oxides with different methods including an improved salt titration method. *Soil Science*, 173(4), 277-286.
- [22] Hasan, D.u.B., Aziz, A.A. & Daud, W.M.A.W. (2012). Using D-optimal experimental design to optimise remazol black B mineralisation by Fenton-like peroxidation. *Environmental Technology*, 33(10), 1111-1121.
- [23] Montgomery, D.C., Runger, G.C. & Hubele, N.F. (2009) *Engineering statistics*, John Wiley & Sons.
- [24] Khosravi, R., Moussavi, G., Ghaneian, M.T., Ehrampoush, M.H., Barikbin, B., Ebrahimi, A.A. & Sharifzadeh, G. (2018). Chromium adsorption from aqueous solution using novel green nanocomposite: Adsorbent characterization, isotherm, kinetic and thermodynamic investigation. *Journal of Molecular Liquids*, 256, 163-174.
- [25] Igerase, E., Osifo, P. & Ofomaja, A. (2017). Chromium (VI) ion adsorption by grafted cross-linked chitosan beads in aqueous solution—a mathematical and statistical modeling study. *Environmental Technology*, 38(24), 3156-3166.
- [26] Pradhan, J., Das, S.N. & Thakur, R.S. (1999). Adsorption of hexavalent chromium from aqueous solution by using activated red mud. *Journal of Colloid and Interface Science*, 217(1), 137-141.
- [27] Bhatti, I.A., Ahmad, N., Iqbal, N., Zahid, M. & Iqbal, M. (2017). Chromium adsorption using waste tire and conditions optimization by response surface methodology. *Journal of Environmental Chemical Engineering*, 5(3), 2740-2751.
- [28] Zhao, J., Liu, J., Li, N., Wang, W., Nan, J., Zhao, Z. & Cui, F. (2016). Highly efficient removal of bivalent heavy metals from aqueous systems by magnetic porous Fe<sub>3</sub>O<sub>4</sub>-MnO<sub>2</sub>: Adsorption behavior and process study. *Chemical Engineering Journal*, 304, 737-746.
- [29] Mourabet, M., El Rhilassi, A., El Boujaady, H., Bennani-Ziatni, M., El Hamri, R. & Taitai, A. (2012). Removal of fluoride from aqueous solution by adsorption on Apatitic tricalcium phosphate using Box–Behnken design and desirability function. *Applied Surface Science*, 258(10), 4402-4410.
- [30] Mondal, N.K., Samanta, A., Chakraborty, S. & Shaikh, W.A. (2018). Enhanced chromium (VI) removal using banana peel dust: isotherms, kinetics and thermodynamics study. *Sustainable Water Resources Management*, 4(3), 489-497.
- [31] Karthik, R. & Meenakshi, S. (2015). Removal of Cr (VI) ions by adsorption onto sodium alginate-polyaniline nanofibers. *International Journal of Biological Macromolecules*, 72, 711-717.
- [32] Sarin, V. & Pant, K.K. (2006). Removal of chromium from industrial waste by using eucalyptus bark. *Bioresource Technology*, 97(1), 15-20.
- [33] Kataria, N. & Garg, V. (2018). Optimization of Pb (II) and Cd (II) adsorption onto ZnO nanoflowers using central composite design: isotherms and kinetics modelling. *Journal of Molecular Liquids*, 271, 228-239.
- [34] Zbair, M., Anfar, Z., Ahsaine, H.A., El Alem, N. & Ezahri, M. (2018). Acridine orange adsorption by zinc oxide/almond shell activated carbon composite: operational factors, mechanism and performance optimization using central composite design and surface modeling. *Journal of Environmental Management*, 206, 383-397.
- [35] Reddy, Y. S., Magdalane, C. M., Kaviyarasu, K., Mola, G. T., Kennedy, J., & Maaza, M. (2018). Equilibrium and kinetic studies of the adsorption of acid blue 9 and Safranin O from aqueous solutions by MgO decorated FLG coated Fuller's earth. *Journal of Physics and Chemistry of Solids*, 123, 43-51.